ELSEVIER

Journal of Electroanalytical Chemistry 512 (2001) 83–91

Journal of Electroanalytical Chemistry

www.elsevier.com/locate/jelechem

Faradaic impedance titration of pure 3-mercaptopropionic acid and ethanethiol mixed monolayers on gold

Kyuwon Kim, Juhyoun Kwak *

Department of Chemistry, Korea Advanced Institute of Science and Technology, 373-1 Kusong-dong Yusong-gu, Taejon 305-701, South Korea

Received 29 December 2000; received in revised form 14 June 2001; accepted 14 June 2001

Abstract

Interfacial proton transfer reactions of pure 3-mercaptopropionic acid (MPA) and ethanethiol (EtSH) mixed self-assembled monolayers (SAMs) have been studied using the faradaic impedance titration method. The $Fe(CN)_6^{3-}$ is used to probe the charge development of the terminal –COOH group of the monolayers. The charge-transfer resistance (R_{ct}) is measured with the monolayer composition, adsorption coverage, and the ionic strength of pH solution. The surface pK determined for the pure MPA is 6.0 at a monolayer coverage and 0.1 M ionic strength. The in-plane electrostatic force effect, which causes a broadening of the titration curves, on the surface pK for the MPA SAM is not significant at an ionic strength over 0.1 M. The pK value for the pure MPA SAM shifts negatively as the surface coverage decreases, indicating that the in-plane interactions between acids and the hydrophobicity surrounding acids decrease at the same time. When the pure MPA SAM is compared with the EtSH mixed SAM, the surface pK of the mixed SAM is larger than that of the pure SAM. Such positive pK shifts are more pronounced at the pure MPA SAM with a lower coverage. This implies that the pK shifts of sparsely adsorbed acidthiol SAM are more sensitive to the introduction of hydrophobicity than to the decrease of the in-plane interactions.

Keywords: Faradaic impedance titration; Surface pK; Self-assembled monolayers; Proton transfer; Charge-transfer resistance; 3-Mercaptopropionic acid (MPA)

1. Introduction

There has been enormous interest in designing highly selective interfaces for use in sensing and separation technology. Chemically modified interfaces such as alkanethiol self-assembled monolayers (SAMs) on gold have been studied intensively in recent years because they form easily and exhibit robust and ordered structures [1,2].

Interfacial proton transfer studies are crucial to understand and control acid/base properties of surface-confined molecules and are essential to applications including fundamental studies of interfacial phenomena, such as wetting [3], biological interactions [4,5], and the development of novel molecular sensing architectures [6,7]. Various methods have been used to measure the acidity of surface-adsorbed ω-funtionalized alkanethiols terminated by acidic or basic groups. These include differential interfacial capacitance [8–10], contact angle [3,11–13], mass change [14–16], force titration [17–21], surface-enhanced Raman scattering [22], a laser-induced temperature jump [23], and amperometric methods [24–26]. Amperometric or electrochemical methods monitor the influence of the charge of the acidic or basic terminal group of SAMs on the current response of cyclic voltammetry (CV) for an electroactive probe molecule (e.g. $Fe(CN)_6^{3-}$). The redox response of the probe molecule changes with solution pH, because the extent of repulsion between the probe and the terminal group depends on the pH. Although observation of the current is simple and convenient, it may often be insensitive due to double-layer charging and changes of charge density in the monolayer during the charge-transfer reaction.

Impedance spectroscopy describes more explicitly the faradaic or nonfaradaic behavior, such as currents due to diffusion, double-layer charging, resistance of the

* Corresponding author. Tel.: +82-42-869-2833; fax: +82-42-869-2810.

E-mail address: jhkwak@kaist.ac.kr (J. Kwak).

0022-0728/01/$ - see front matter
PII: S0022-0728(01)00588-5

solution (R_s) and charge transfer (R_{ct}), which occur in the SAMs [27]. Faradaic impedance spectroscopy techniques using a redox probe molecule can reveal a dependence of electron transfer resistance on the charge developing in terminal acid or base groups of SAMs during titration. The R_{ct} is measured and plotted with solution pH, and this method is termed 'faradaic impedance titration.' Previous studies on the pH dependence of the R_{ct} at acid or base terminated SAMs using impedance spectroscopy have been reported [28–30]. However, there has not been a detailed quantitative faradaic impedance study on the pK behavior under various experimental parameters.

In the present study, we describe the surface pK dependence upon the acid coverage, composition, and the ionic strength using faradaic impedance titration. MPA and Ethanethiol (EtSH) are selected for this investigation because their SAMs do not perfectly block the charge-transfer reactions of electroactive molecules due to their short chains, in spite of having ordered structures on gold [31,32]. Thus their SAMs provide a favorable interface for faradaic impedance titration. Moreover, understanding of the proton transfer at the MPA SAM is important since this SAM has been shown to serve as an adhesion layer for positive charged proteins such as cytochrome *c* [33]. Ethanethiol is introduced to change the composition of the surfaces. Mirkin and coworkers incorporated EtSH into ferrocenylazobenzenebutanethiol and cysteamine monolayers for effective dilution [34,35]. The pK values of pure ω-funtionalized SAMs with a high and low coverages are compared, respectively, with those of the corresponding mixed SAMs, and a comparative analysis of the respective pK shifts is presented. Various studies on SAM-modified electrodes have shown that changing the active area or the charged state of the electrodes can control the electron transfer rate of redox active molecules [36,37]. However, only a few reports have described controlling the extent of the proton transfer reaction. Very recently, Shimazu and coworkers reported that varying the electrode potential could change the surface pK of 15-mercaptohexadecanoic acid [16]. Herein, we wish to demonstrate that the manipulation of surface coverage and composition can control the proton transfer properties (i.e. surface pK) of acid SAMs.

2. Experimental

2.1. Chemicals

3-Mercaptopropionic acid (MPA), EtSH, sodium perchlorate, sodium hydroxide, perchloric acid, phosphoric acid (Aldrich), potassium ferricyanide (Sigma), and absolute ethanol (Merck) were reagent grade or better and all were used as received. Ultra-pure water (>18 MΩ) from a Modulab water system (US Filter Corp.) was used throughout this work. All glassware was cleaned for 6 h in Nochromix (Godax Lab., Inc.) cleaning solution, 6 h in concentrated HNO_3, and then rinsed with ultra-pure water.

2.2. Preparations of electrodes and SAMs

All gold plate electrodes were prepared by deposition (0.7–1 Å s^{-1}) of ca. 300 nm of gold ($>99.99\%$) on glass. The pressure during evaporation was typically below 10^{-6} Torr. Glass plates were pretreated with a ca. 20–30 nm adhesive layer of chromium (99.99%).

For a SAM coated gold electrode, a clean gold plate was placed in an absolute ethanol solution containing 4 mM of pure MPA or MPA + EtSH at room temperature. After soaking, the electrode was rinsed with pure ethanol and water to remove physically adsorbed molecules, dried in an Ar stream, and then transferred to the electrochemical cell.

2.3. Measurements of cyclic voltammograms and impedances

An electrolyte solution having a constant ionic strength was prepared using the method of Smalley et al. [23]. The initial pH was ca. 2.1 for either 0.1 or 0.5 M $NaClO_4$ + 0.01 M H_3PO_4. The higher pH was adjusted by the addition of either 0.11 M NaOH (for 0.1 M ionic strength) or 0.11 M NaOH + 0.39 M $NaClO_4$ (for 0.5 M ionic strength) and was measured with a calibrated pH meter (HI8418, Hanna Instruments). The electrochemical cell was filled with the pH-adjusted electrolyte solution of 0.5 mM $K_3Fe(CN)_6$ and deoxygenated with Ar.

Cyclic voltammetry was performed using an AUTOLAB 10 (Eco Chemie, Netherlands) interfaced with a personal computer. The geometrical area of the gold plate working electrode was 0.40 cm^2. A standard three-electrode cell was used with a $Hg \mid Hg_2SO_4 \mid K_2SO_4$ (sat) electrode (MSE) as the reference electrode and a Pt wire counter electrode. Using the frequency response analyzer of the AUTOLAB 10, the impedance at the formal potential of the redox probe, which was superimposed on 5 mV rms sinusoidal potential modulations, was measured for 30 frequencies from 50 mHz to 2 kHz. The data at different pH values are represented in the complex plane; Nyquist plots (Z'' vs. Z', Z'' = imaginary impedance and Z' = real impedance). The respective semicircle diameters correspond to the interfacial R_{ct} of which values are calculated from the nonlinear least-squares (NLLS) fitting program of AUTOLAB 10. The impedance spectra are fitted to a modified Randles equivalent electrical circuit for both bare and SAM adsorbed electrodes, including the solu-

tion resistance, R_s, a constant phase element (CPE), the charge-transfer resistance, R_{ct}, and Warburg impedance, Z_W. Instead of an ideal capacitor, the CPE is used to compromise errors due to microscopic roughness and atomic scale inhomogeneity in surfaces [38]. From the regression, the charge-transfer resistance (R_{ct}) is obtained and plotted with various pH values.

3. Results and discussion

3.1. Charge-transfer resistance (R_{ct}) of $Fe(CN)_6^{3-}$ at bare gold electrodes

We used $Fe(CN)_6^{3-}$ as an electrochemically active probe molecule to investigate the charge-transfer resistance of the pure MPA and MPA + EtSH SAMs under the various experimental conditions. Bulk phase electrochemistry of the redox probe molecule on a bare electrode is contrasted with that for the SAM-modified Au electrodes. For the bare electrode, CV for 0.5 mM $K_3Fe(CN)_6$ at various pH values was performed. All of the CVs exhibit electrochemically reversible features regardless of the solution pH. The formal potential ($E^{\circ\prime}$) of -0.21 ± 0.01 V is calculated from the midpoint value of the positive and negative peak potentials.

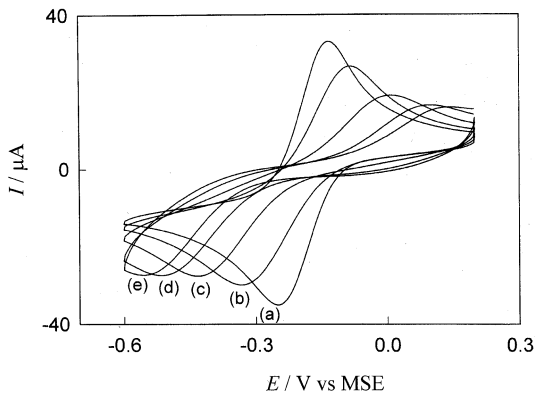

Fig. 1. Cyclic voltammograms for the redox reaction of 0.5 mM $Fe(CN)_6^{3-}$ at pH: (a) 3.5; (b) 4.5; (c) 5.5; (d) 6.5; and (e) 7.5 solutions of 0.1 M ionic strength on a MPA modified gold electrode. Coating time is 60 h. Scan rate is 100 mV s^{-1}.

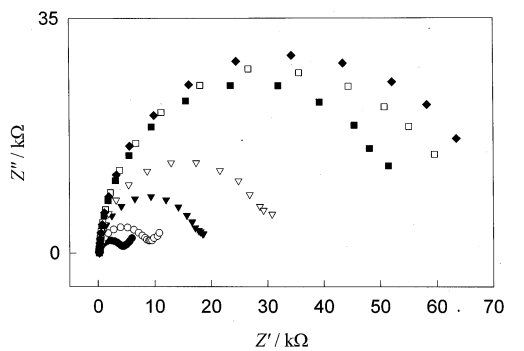

Fig. 2. Complex impedance plots of a MPA modified electrode in the presence of 0.5 mM $Fe(CN)_6^{3-}$ at pH 4.5 (●), 5.0 (○), 5.5 (▼), 6.0 (▽), 6.5 (■), 7.0 (□), and 7.5 (◆) solutions of 0.1 M ionic strength. Coating time is 60 h.

The impedance spectra for the redox reaction of $Fe(CN)_6^{3-}$ were measured at the bare Au electrodes. The change of R_{ct} with varying pH was measured at the formal potential of $Fe(CN)_6^{3-}$. The value is 64 Ω at pH 3.5. As expected from the CVs results, the charge-transfer resistances of the probe molecule do not vary with changing solution pH.

3.2. Determination of surface pK of pure and mixed MPA SAMs on gold

CVs of 0.5 mM $K_3Fe(CN)_6$ in various pH solutions with 0.1 M ionic strength at an electrode modified with pure MPA for 60 h are shown in Fig. 1. At very low pH (pH < 4) the acid group is completely protonated; therefore no electrostatic repulsive interactions between the MPA-modified Au electrode and $Fe(CN)_6^{3-}$ are expected. The repulsive force increased with increased pH, indicating that the carboxylic acid group is gradually deprotonated as the pH increases. Consequently, suppressed and irreversible voltammetric behavior, such as a decrease in the peak current of $Fe(CN)_6^{3-/4-}$ and an increase of peak splitting (ΔE_p, $E_{pa} - E_{pc}$), appears in Fig. 1. The acid group seems to be fully deprotonated in the range over pH 7, because the increment of ΔE_p is markedly lowered in that pH region. Fig. 2 shows that the impedances for the pure MPA SAM increase following modification of the gold electrode and are pH dependent. The dramatic changes of the R_{ct} increment in the spectra make the surface pK of the SAM readily apparent, even without recording a titration curve. The titration curves of the impedance for the pure and mixed MPA monolayers are plotted as a function of solution pH, as shown in Fig. 3. The $pK_{1/2}$ is defined as the pH value when half of the acid is ionized. The values are estimated from the midpoints of inflection of the titration curves, assuming that half the acids are deprotonated at that point. The $pK_{1/2}$ determined for the pure MPA is 6.0. Porter and coworkers suggested that alkanethiol monolayers on gold electrodes were desorbed in alkaline solution through a one electron reductive reaction [39,40] and this phenomenon has been used to measure the surface coverage of alkanethiol [40,41]. We estimated the coverage of the pure MPA SAM in 0.5 M KOH solution using the reductive desorption method without correcting for surface roughness and charging current during the desorption. For 60 h of immersion time, the value is 8.1×10^{-10} mol cm^{-1}, which is consistent with the previous results by other groups [40,41].

There have been theoretical studies for the dependence of surface pK on the surface potential (Ψ)

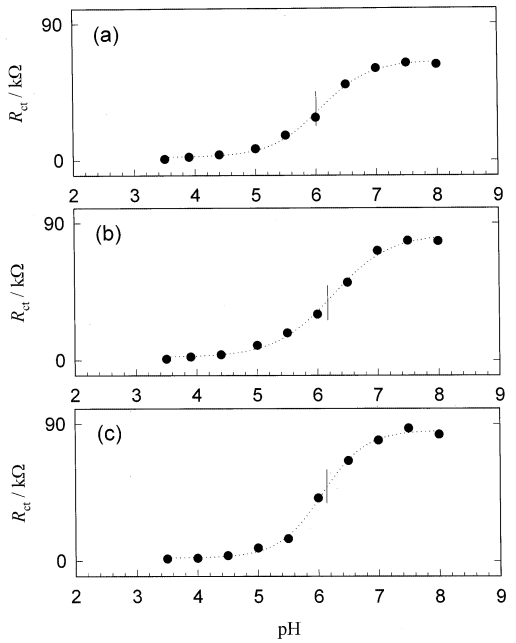

Fig. 3. Faradaic impedance titration curves for: (a) pure MPA; (b) 9:1 (MPA + EtSH) mixed; and (c) 1:1 (MPA + EtSH) mixed SAM. Ionic strength is 0.1 M and coating time is 60 h.

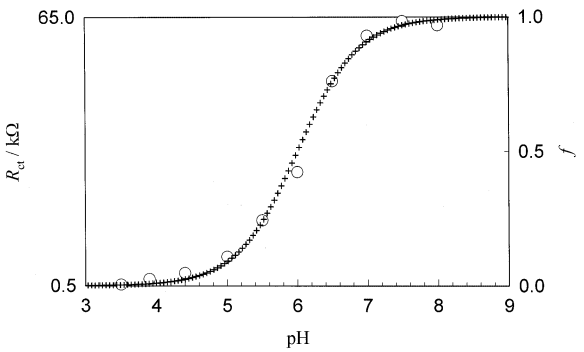

Fig. 4. Experimental plots (○) by faradaic impedance titration for pure MPA SAM and calculated plots (+) based on Eq. (2).

[42,43]. Smith and White assumed that all acid/base groups lie in the common plane, referred to as the 'plane of acid dissociation' (PAD), and defined Ψ as the potential drop between the PAD and the bulk solution [42].

$$\log[f/(1-f)] = \mathrm{pH} - (\mathrm{p}K - F\Psi/2.3RT) \quad (1)$$

where f is the fraction of ionized molecules in the monolayers and K is the dissociation constant of the surface-bound acid when $\Psi = 0$. From Eq. (1) and the above definition of $\mathrm{p}K_{1/2}$, it follows that $\mathrm{p}K_{1/2} = \mathrm{p}K - F\Psi/2.3RT$.

To investigate the in-plane electrostatic force effect on the surface pK, the Ψ dependence of the titration curve has been considered. For this, the titration curve (i.e. R_{ct} vs. pH) is compared with the plot of the theoretical prediction (i.e. f vs. pH). With the increase of f, the surface potential Ψ is shifted to more negative values, because of the increase of the repulsive force between charged acids in a SAM. The Ψ change as a function of f results in the broadening of the titration curve. Neglecting the dependence of Ψ upon f, by replacing $(\mathrm{p}K - F\Psi/2.3RT)$ of Eq. (1) by 6.0, which is the experimentally determined $\mathrm{p}K_{1/2}$ for the pure MPA monolayer, we can rewrite Eq. (1):

$$\log[f/(1-f)] = \mathrm{pH} - 6.0 \quad (2)$$

The titration curve observed experimentally would be broader than the plot by Eq. (2) if the effect on the surface pK were significant [19]. Fig. 4 represents a titration curve from experiment for the pure MPA and a calculated curve based on Eq. (2). The relation between R_{ct} and f is given by $f = (R_{ct} - R_{ct,\,low\,pH})/(R_{ct,\,high\,pH} - R_{ct,\,low\,pH})$. It is surprising that the theoretical consideration by Eq. (2) predicts well the experimental curve from the impedance titration, indicating that Ψ has a constant value of near zero regardless of f (or solution pH) and the repulsive force even at high pH is negligible. The magnitude of the repulsive force may depend on the chain length of acid thiol and the ionic strength of pH solution. Kakiuchi et al. reported that the capacitance titration curve for $HS(CH_2)_6COOH$ SAM broadens by the repulsive force between deprotonated acids at 0.1 M ionic strength [10]. Hu and Bard demonstrated that the force titration curve even for MPA SAM at 0.001 M ionic strength is strongly affected by the surface electrostatic potential [19]. The apparent lack of the effect at 0.1 M ionic strength in our experiment may be explained by the chain length of MPA, which is too short to construct a highly ordered and densely packed monolayer. The high ordering and dense packing, expected at the longer chain acid SAMs, should elevate the repulsive force between the deprotonated acids. Although the adsorption of MPA could not form a highly dense structure due to its short chain length, it is unreasonable to expect that the distance between the nearest neighboring MPA on gold is much longer than 0.5 nm, which is the spacing of closely packed alkanethiols [31], because the estimated monolayer coverage of MPA (8.1×10^{-10} mol cm^{-2}) in our experiments is similar to that of the closely packed SAMs of alkanethiols. The Debye length of $NaClO_4$ at 0.1 M ionic strength is calculated to be ca. 0.96 nm [44, p. 506]. Because this value is larger than that of the MPA spacing on gold, repulsive interactions cannot be completely excluded from the experimental determination of surface pK for MPA SAM and its shift. The Ψ independence of the titration curve is not fully understood. Nonetheless, it would be logical to suppose that the electrostatic force effect on the surface pK at an ionic strength of 0.1 M is negligible at least for MPA SAM, since we could not observe

the broadening of titration curves in this experiment. Therefore, it is likely that the effect is more negligible in the titration for pure MPA SAM under the conditions of lower coverage or higher ionic strength. From the small effect, we can approximate the $pK_{1/2}$ as representing the pK.

Fig. 4 also indicates that the relation between R_{ct} and the fraction of ionized molecules (f) is linear in the entire pH range tested. Comparing R_{ct} to the resistance of a conductor of uniform cross-section, f would be inversely proportional to the cross-section area. This relation can be also explained by the Frumkin effect [44, pp. 540–544]. The ionizable acid group of the MPA SAM is assumed to be at the inner Helmholtz plane [45]. The position of the closest approach of the $Fe(CN)_6^{3-}$, undergoing a redox reaction, is the outer Helmholtz plane. The changes in the reaction kinetics at a constant applied electrode potential are based on changes in the potential at the outer Helmholtz plane (ϕ) with pH because the pH affects the ionization of acids, which changes ϕ. Accordingly, R_{ct} at the outer Helmholtz plane is proportional to f, which increases as the pH increases.

The determined surface pK value of 6.0 in Fig. 3(a) shifts about 1.3 pH units in the positive direction compared with ca. 4.7 for bulk alkanoic acid in 0.1 M $NaClO_4$ solution [23]. Such positive shifts of surface pK for the pure MPA SAM are consistent with the results obtained from other methods. Using atomic force microscopy, Hu and Bard reported a pK of 8.0 for MPA SAM by double-layer force measurement [19]. Shimazu et al. used a quartz crystal microbalance, and obtained a surface pK of 5.8 for MPA [15]. Electrochemical titration by Zhao et al. gave a value of 5.2 [26]. These substantial positive shifts by less favorable deprotonation of the surface-confined carboxylic acid group have been rationalized by three different factors. The first is the large electrostatic repulsions between neighboring ionized carboxylate groups that is predicted by double-layer effect [43,45]. This probably does not substantially affect the pK shifts, at least in this experiment, since the surface potential dependence of the titration curve is negligible as discussed above. The second is the ion solvation effects due to the existence of an inner layer with a low dielectric constant [3]. The influences of these two factors on the shifts of the formal potential of ferrocenyl–alkanethiol SAMs have been previously reported [46]. The third is the hydrogen bond formations between terminal –COOH groups. Carboxylic acid groups in the SAMs are known to form in-plane hydrogen bonding [47].

Fig. 3 also shows that the pK shifts with the introduction of EtSH are not significant. The report of Kakiuchi et al. for 1:1 mixed SAM of $HS(CH)_5COOH$ and $SH(CH)_2CH_3$ demonstrated that the mixing of alkanethiols causes a decrease of 0.5 pH unit in the surface pK [10]. Creager and Clarke also showed that the pK shifts slightly to a lower value when the coverage ratio of acid in mixed SAMs decreases [3]. Such previous observations reflect that the reduction of in-plane interactions such as the hydrogen bond formations and the repulsive interactions between acids are superior to the increase of hydrophobicity. However, the trend has not been observed in this MPA system. This might be attributed to a higher dielectric constant and lower intermolecular interactions at the MPA monolayer than in longer chain acids. Since MPA is probably too short to form a highly ordered structure, the in-plane interactions, resulting in the positive shifts of pK, may be smaller than those of the longer chain acids. Consequently, the MPA SAM is more sensitive to lowering of the dielectric constant than longer chain acid SAMs. This argument is in accordance with the lack of an electrostatic effect on the pK of MPA SAM described above. It has been previously reported that the decreasing chain length gives rise to a reduction in positive shifts of surface pK [10,15].

3.3. Surface coverage effects on surface pK shifts at pure and mixed MPA SAMs on gold

Low surface coverage of MPA should reduce the formation of hydrogen bonds and the intermolecular repulsions between the acid terminal groups of monolayers. A MPA SAM with lower acid coverage could be prepared by dilution with alkanethiol or shorter time immersion of the electrode in acid thiol solutions. The first method can be employed to eliminate in-plane interactions. However, as mentioned earlier, co-adsorbed alkanethiol brings about a much more hydrophobic surrounding for the acid groups, shifting the pK in the positive direction (see Scheme 1(a)). On the other hand, the second approach reduces the in-plane interactions as shown in Scheme 1(b), and the hydrophobicity also decreases. At the same time, the resulting low density of carboxylate anions favors the access of negatively charged $Fe(CN)_6^{3-}$ to the defects in the surface, thus resulting in a diminished R_{ct}. In this section, controlling coverage experiments by the second method are performed by soaking a gold electrode with different coating times in the same solution concentration.

The titration curves for the pure and mixed SAMs are plotted in Fig. 5. The R_{ct} of the pure SAM decreased, compared with that of 60 h immersion, indicating a lower coverage due to reduced soaking time. By the reductive desorption, the adsorption coverage of the pure MPA is measured as 6.8×10^{-10} mol cm^{-2} at 1 h immersion, which is ca. 85% of the value of 60 h immersion. This submonolayer coverage implies that the surface adsorption kinetics of MPA are much slower than that of longer chain acids despite the relatively high concentration (4 mM) of the coating

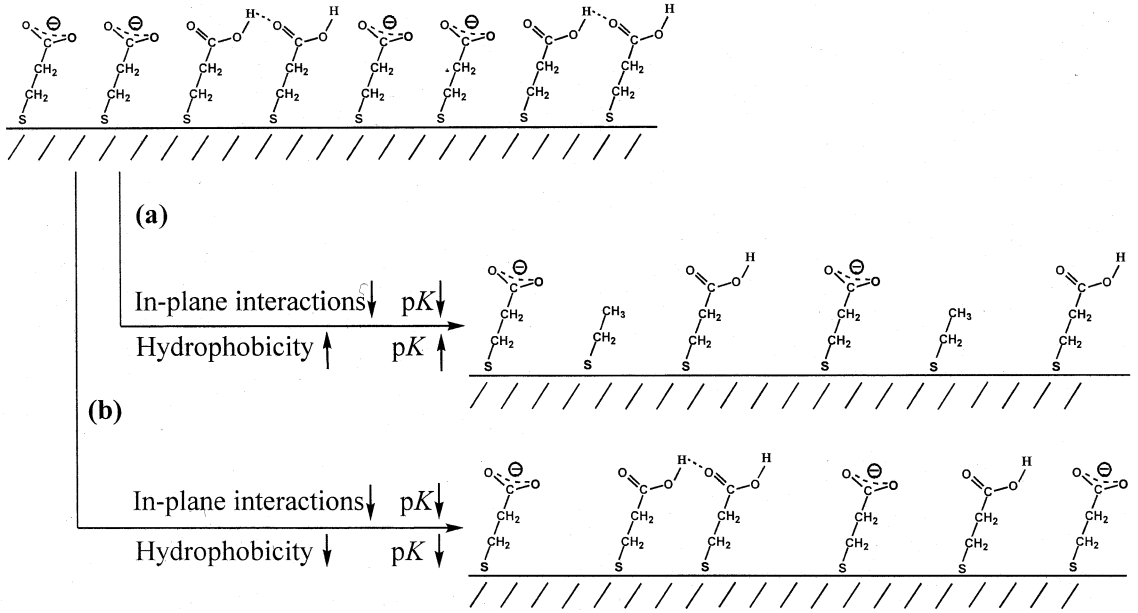

Scheme 1.

solution. Hu and Bard examined the adsorption of $SH(CH_2)_{10}COOH$ on gold, formed in alkaline solution, using atomic force microscopy [48]. They observed that the surface coverage reached 90% of the monolayer coverage occurring within 1 h by soaking 0.5 mM solution of the acid thiol. This coverage discrepancy is explained by chain length dependent adsorption kinetics [49,50].

The determined pK is 5.2 for the pure SAM. Comparing the titration curve for the pure MPA in Fig. 5(a) with the plot of f versus pH by the equation:

$$\log[f/(1-f)] = \mathrm{pH} - 5.2 \quad (3)$$

The slopes of the two curves match well, as is shown in Fig. 4. This deficient Ψ dependence of the experimental titration curve is more easily accepted at the submonolayer coverage system because the extent of repulsion between acids on gold is lower than that of the fully covered MPA SAM. For the two pure SAMs prepared for different coating times, the pK shift from 6.0 to 5.2 with decreasing time may be attributed to the sparser adsorption of MPA. This sparsity gives rise not only to the decline of intermolecular in-plane interactions between acids but also the reduction of the hydrophobicity of the microenvironments. Kakiuchi and co-workers described the peak potential shifts of reductive desorption for a pure MPA SAM influenced by surface coverage [41]. They interpreted the positive potential shifts with decreasing coverage as lowered intermolecular interaction (e.g. chain–chain interactions and electrostatic interactions) between carboxylate groups in sparsely adsorbed MPA monolayers.

For the mixed SAMs in Fig. 5, the pK values are 5.8 regardless of the mixing ratio in the coating solution. The pK increase from 5.2 for the pure SAM to 5.8 for the mixed SAMs is greater than that of SAMs prepared from 60 h of immersion. This result is reasonable because the acid density of the mixed SAMs from 1 h immersion is not higher than that of the pure SAM from 1 h immersion and therefore the co-adsorbed EtSH mostly serves to increase the hydrophobicity rather than to reduce the in-plane interactions by diluting the acids. In other words, when the MPA SAM

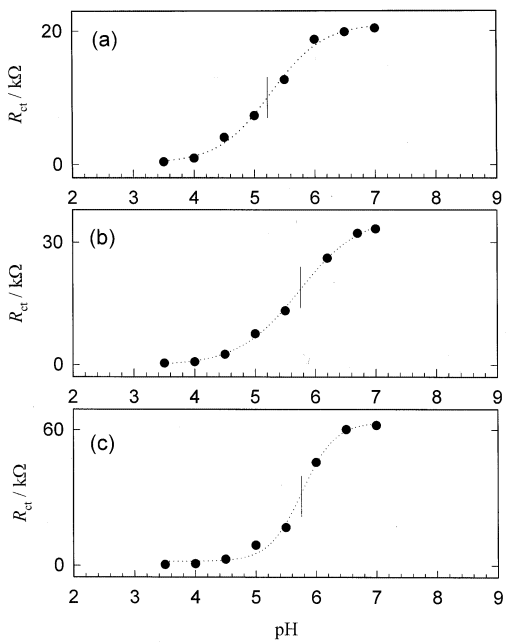

Fig. 5. Faradaic impedance titration curves for: (a) pure MPA; (b) 9:1 (MPA + EtSH) mixed; and (c) 1:1 (MPA + EtSH) mixed SAM. Ionic strength is 0.1 M and coating time is 1 h.

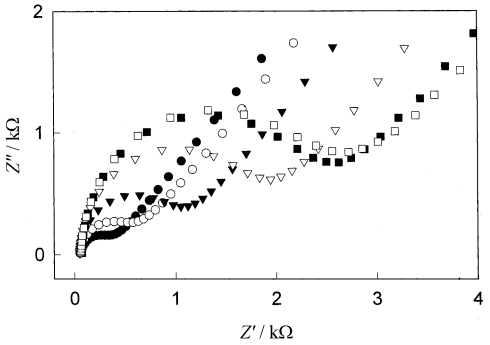

Fig. 6. Complex impedance plots of a MPA modified electrode in the presence of 0.5 mM $Fe(CN)_6^{3-}$ at pH 3.5 (●), 4.0 (○), 4.5 (▼), 5.0 (▽), 5.5 (■), and 6.0 (□) solutions of 0.5 M ionic strength. Coating time is 60 h.

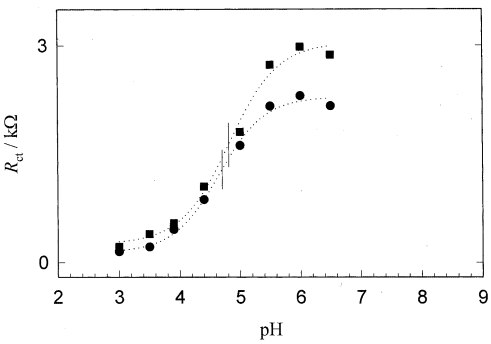

Fig. 7. Faradaic impedance titration curves for pure MPA (●) and 9:1 (MPA + EtSH) mixed (■) SAM. Ionic strength is 0.5 M and coating time is 60 h.

with a low coverage is co-adsorbed with EtSH, the pK increase is enhanced further (compare with Fig. 3). It is instructive that the surface pK changes with adjustable parameters such as the coverage and composition of surface, because this means that we can control the surface pK by manipulating these parameters. The control of the pH sensitive charge properties of acid/base-terminated monolayers on electrodes is essential to develop a highly selective molecular sensing method based on the interfacial electron transfer reaction [6,51]. Controlling the surface pK is expected to provide an effective control of these charge properties.

3.4. Ionic strength effects on proton transfer reactions of pure and mixed MPA SAMs on gold

While the pK of carboxylic acid in the bulk solutions is not sensitive to changes in ionic strength, the pK of surface-adsorbed acid is highly dependent upon the changes [10,21,23]. Increased counterions of electrolytes screen the formation of in-plane hydrogen bonding between acids [21] and therefore the surface pK shifts can be caused by the association of counterions with the $-COO^-$ group of MPA. At the starting point of ionization, the ionized acid seems to take part in hydrogen bonding in the plane of acid dissociation. Since this bonding would make it difficult to dissociate the acids, the pK shifts to a higher value. At a higher ionic strength, these strong in-plane hydrogen bondings are blocked due to the formation of ion pairs between $-COO^-$ and counterions, and adjacent neutral acids can be more easily deprotonated even at a lower pH. In addition, at the acid SAM with a high coverage, the interfacial potential growth owing to the intermolecular repulsion can be screened by counterions. In that situation, the concentration of counterions may be much higher at the interface of carboxylate than in the bulk. The Donnan potential developed at the interface, which is caused by the concentration gradient of counterions, changes with the degree of acid deprotonation because the ions migrate toward or away from the acid plane in order to compensate for the charge development. This charge compensation reduces the repulsive interactions between the deprotonated acid terminals, and is favored with increased ionic strength, leading to a high concentration of counterions. Consequently, the higher ionic strength shifts the surface pK at the lower ionic strength to a lower value.

To confirm the ionic strength effects, a faradaic impedance titration was performed for the pure or the mixed SAMs at different electrolyte concentrations. Fig. 6 shows the impedance plots acquired in a 0.5 M ionic strength solution; faster electron transfer kinetics of $Fe(CN)_6^{3-}$ are observed, compared to those in a 0.1 M solution. These plots exhibit typical features for the semi-infinite diffusion process; semicircles in the high frequency region and Warburg impedance lines in the low frequency area. A greatly reduced R_{ct} indicates that the increase of counterion concentration contributes to the elimination of not only the in-plane interaction at the SAM but also the repulsion between $Fe(CN)_6^{3-}$ and the carboxylate anions. The influence of the ionic strength on the reaction kinetics may also be explained by the Frumkin effect [44, pp. 540–544]. Increase of the ionic strength decreases the absolute value of the potential of the outer Helmholtz plane ($|\phi|$) and decreases R_{ct}.

Fig. 7 represents the titration curves for the two series of impedance behavior. The pK values for the pure and 9:1 mixed SAM are both $\sim$4.7. As expected, an increased ionic strength resulted in negative pK shifts from those in 0.1 M ionic strength. This decrease of ca 1.4 pH units is larger than the results previously measured for longer chain acids by other groups. Smalley et al. found shifts from 5.7 to 4.4 for 11-mercaptoundecanoic acid (MUA) by changing the ionic strength from 0.1 to 1.0 M [23]. Kakiuchi et al. also observed a decrease from 9.9 to 9.6 for $HS(CH_2)_6COOH$ SAM with increased ionic strength from 0.01 to 0.1 M [10]. The sensitive response of the

pure MPA is interpreted to be due to the provision of a more permeable membrane for the counterions than MUA or $HS(CH_2)_6COOH$. It is interesting that the pK obtained of 4.7 is the same for the bulk acid, meaning that additional interactions and the hydrophobicity of the microenvironments caused by monolayer formations have been perfectly eliminated by the counterions. The electrostatic force effect on the curve for the pure MPA SAM in Fig. 7 is also negligible. The repulsive force between acids would be further removed than that in 0.1 M ionic strength solution because the Debye length of the electrolytes is ca. 0.43 nm at 0.5 M ionic force solution and it is shorter than the assumed distance of 0.5 nm between MPA molecules on gold.

4. Conclusions

We have studied the effects of the monolayer composition, the surface coverage and the ionic strength of the pH solution on the proton transfer reactions at the electrochemical interface of pure MPA and EtSH mixed SAMs using faradaic impedance titration. It has been shown that the impedance titration is a very sensitive technique in revealing these effects. In our impedance titration, the in-plane electrostatic force effect on the surface pK of MPA SAM at ionic strengths over 0.1 M is not significant. Accordingly, the major factors that affect the shift of surface pK for MPA SAM in this study are assumed to be the hydrogen bond formations between acids and the dielectric properties surrounding acids. A comparative study of the respective pK shifts has been described for pK values of two pure ω-funtionalized SAMs with high and low coverages and the corresponding mixed SAMs. This revealed that the surface pK of sparsely adsorbed acidthiols is more sensitive to the introduction of hydrophobicity than to the reduction of intermolecular interactions such as hydrogen bonding or repulsive interactions. These experiments enable us to control the pH sensitive charge properties of the acid SAM by adjusting the surface coverage and composition of the monolayer and to understand the proton transfer properties of the MPA SAM in the presence of a faradaic process.

Acknowledgements

This work was supported by the Korea Science and Engineering Foundation through the MICROS center at KAIST and partially supported by the Brain Korea 21 Project in 2001.

References

[1] L.H. Dubois, R.G. Nuzzo, Annu. Rev. Phys. Chem. 43 (1992) 437.
[2] A. Ulman, Chem. Rev. 96 (1996) 1533.
[3] S.E. Creager, J. Clarke, Langmuir 10 (1994) 3675.
[4] G.P. Lopez, M.W. Albers, S.L. Schreiber, R. Carroll, E. Peralta, G.M. Whitesides, J. Am. Chem. Soc. 115 (1993) 5877.
[5] R. Singhvi, A. Kumar, G.P. Lopez, G.N. Stephanopoulos, D.I.C. Wang, G.M. Whitesides, D.E. Ingber, Science 264 (1994) 696.
[6] E. Katz, M. Lion-Dagan, I. Willner, J. Electroanal. Chem. 408 (1996) 107.
[7] I. Willner, E. Katz, Angew. Chem. Int. Ed. Engl. 39 (2000) 1180.
[8] M.A. Bryant, R.M. Crooks, Langmuir 9 (1993) 385.
[9] H.S. White, J.D. Peterson, Q. Cui, K.J. Stevenson, J. Phys. Chem. B 102 (1998) 2930.
[10] T. Kakiuchi, M. Iida, S. Imabayashi, K. Niki, Langmuir 16 (2000) 5397.
[11] C.D. Bain, G.M. Whitesides, Langmuir 5 (1989) 1370.
[12] T.R. Lee, R.L. Carey, H.A. Biebuyck, G.M. Whitesides, Langmuir 10 (1994) 741.
[13] R.C. Chatelier, C.J. Drummond, D.Y.C. Chan, Z.R. Vasic, T.R. Gengenbah, H.J. Griesser, Langmuir 11 (1995) 4122.
[14] J. Wang, L.M. Frostman, M.D. Ward, J. Phys. Chem. 96 (1992) 5224.
[15] K. Shimazu, T. Teranishi, K. Sugihara, K. Uosaki, Chem. Lett. (1998) 669.
[16] K. Sugihara, K. Shimazu, K. Uosaki, Langmuir 16 (2000) 7101.
[17] D.V. Vezenov, A. Noy, L.F. Rozsnyai, C.M. Lieber, J. Am. Chem. Soc. 119 (1997) 2006.
[18] E.W. van der Vegte, G. Hadziioannou, J. Phys. Chem. B 101 (1997) 9563.
[19] K. Hu, A.J. Bard, Langmuir 13 (1997) 5114.
[20] H. Zhang, H.X. He, J. Wang, T. Mu, Z.F. Liu, Appl. Phys. A 66 (1998) S269.
[21] D.A. Smith, M.L. Wallwork, J. Zhang, J. Kirkham, C. Robinson, A. Marsh, M. Wong, J. Phys. Chem. B 104 (2000) 8862.
[22] H.Z. Yu, N. Xia, Z.F. Liu, Anal. Chem. 71 (1999) 1354.
[23] J.F. Smalley, K. Chalfant, S.W. Feldberg, T.M. Nahir, E.F. Bowden, J. Phys. Chem. B 103 (1999) 1676.
[24] Q. Cheng, A. Brajter-Toth, Anal. Chem. 68 (1996) 4180.
[25] L.A. Godinez, R. Castro, A.E. Kaifer, Langmuir 12 (1996) 5087.
[26] J. Zhao, L. Luo, X. Yang, E. Wang, S. Dong, Electroanalysis 11 (1999) 1108.
[27] R.P. Janek, W.R. Fawcett, A. Ulman, Langmuir 14 (1998) 3011.
[28] C. Saby, B. Ortiz, G.Y. Champagne, D. Bélanger, Langmuir 13 (1997) 6805.
[29] V. Molinero, E.J. Calvo, J. Electroanal. Chem. 445 (1998) 17.
[30] J. Liu, L. Cheng, B. Liu, S. Dong, Langmuir 16 (2000) 7471.
[31] M.J. Giz, B. Duong, N.J. Tao, J. Electroanal. Chem. 465 (1999) 72.
[32] M.J. Esplandiú, H. Hagenström, D.M. Kolb, Langmuir 17 (2001) 828.
[33] R.A. Clark, E.F. Bowden, Langmuir 13 (1997) 559.
[34] D.J. Campbell, R.H. Brian, C.H. John, R.P. Van Duyne, C.A. Mirkin, J. Am. Chem. Soc. 118 (1996) 10211.
[35] W.B. Caldwell, K. Chen, C.A. Mirkin, S.J. Babinec, Langmuir 9 (1993) 1945.
[36] A.E. Kasmi, J.M. Wallace, E.F. Bowden, S.M. Binet, R.J. Linderman, J. Am. Chem. Soc. 120 (1998) 225.

[37] T.A. Jones, G.P. Perez, B.J. Johnson, R.M. Crooks, Langmuir 11 (1995) 1318.
[38] Z. Kerner, T. Pajkossy, Electrochim. Acta 46 (2000) 207.
[39] M.M. Walczak, D.D. Pnpenoe, R.S. Deinhammer, B.D. Lamp, C. Chung, M.D. Porter, Langmuir 7 (1991) 2687.
[40] C.A. Widrig, C. Chung, M.D. Porter, J. Electroanal. Chem. 310 (1991) 335.
[41] S. Imabayashi, M. Iida, D. Hobara, Z.Q. Feng, K. Niki, T. Kakiuchi, J. Electroanal. Chem. 428 (1997) 33.
[42] C.P. Smith, H.S. White, Langmuir 9 (1993) 1.
[43] R. Andreu, W.R. Fawcett, J. Phys. Chem. 98 (1994) 12753.
[44] A.J. Bard, L.R. Faulkner, Electrochemical Methods: Fundamentals and Applications, Wiley, New York, 1980, p. 506 and pp. 540–544.
[45] W.R. Fawcett, M. Fedurco, Z. Kováová, Langmuir 10 (1994) 2403.
[46] G.K. Rowe, S.E. Creager, J. Phys. Chem. 98 (1994) 5500.
[47] R.M. Crooks, L. Sun, C. Xu, S.L. Hill, A.J. Ricco, Spectroscopy 8 (1993) 28.
[48] K. Hu, A.J. Bard, Langmuir 14 (1998) 4790.
[49] C.D. Bain, E.B. Troughton, Yu.-T. Tao, J. Evall, G.M. Whitesides, R.G. Nuzzo, J. Am. Chem. Soc. 111 (1989) 321.
[50] K.A. Peterlinz, R. Georgiadis, Langmuir 12 (1996) 4731.
[51] T. Komura, T. Yamaguchi, K. Takahashi, H. Teragawa, J. Electroanal. Chem. 481 (2000) 183.